ELSEVIER

CrossMark

BRACHYTHERAPY

Brachytherapy 13 (2014) 618–626

Experimental determination of the Task Group-43 dosimetric parameters of the new I25.S17plus ^{125}I brachytherapy source

Argyris Moutsatsos[1], Evaggelos Pantelis[1], Panagiotis Papagiannis[1,*], Dimos Baltas[2]

[1]*Medical Physics Laboratory, Medical School, University of Athens, Athens, Greece*
[2]*Department of Medical Physics & Engineering, Sana Klinikum, Offenbach, Germany*

ABSTRACT

PURPOSE: To present experimental dosimetry results for the new IsoSeed I25.S17plus ^{125}I brachytherapy source, in fulfillment of the American Association of Physicists in Medicine recommendation for, at least one, experimental dosimetry characterization of new low-energy seeds before their clinical implementation.

METHODS AND MATERIALS: A batch of 100 LiF thermoluminescent dosimeter (TLD)-100 microcubes was used for the experimental determination of the dose-rate constant, radial dose, and anisotropy functions, in irradiations performed using two Solid Water phantoms. Monte Carlo (MC) simulations were used to determine appropriate correction factors that account for the use of Solid Water as a phantom material instead of liquid water and for the different energy response of the TLD dosimeters in the experimental ^{125}I photon energies relative to the 6 MV x-ray photon beam used for the TLD calibration. Measurements were performed for four I25.S17plus seeds; one with direct traceability of air-kerma strength calibration to National Institute of Standards and Technology and three with secondary National Institute of Standards and Technology traceability.

RESULTS: A mean dose-rate constant, Λ, of 0.956 $\pm$ 0.043 cGy h^{-1} U^{-1} was experimentally determined for the I25.S17plus source, which agrees within uncertainties with the MC result of 0.925 $\pm$ 0.013 cGy h^{-1} U^{-1} calculated independently for the same seed model in a previous study. Agreement was also observed between the measured and the MC-calculated radial dose and anisotropy function values.

CONCLUSIONS: Experimental dosimetry results for the I25.S17plus ^{125}I source verify corresponding independent MC results in the form of Task Group-43 dosimetry parameters. The latter are found in agreement within uncertainties with sources of similar design incorporating a silver marker, such as the Oncura OncoSeed Model 6711.

Keywords: ^{125}I seed; TLD; Dosimetry; Task Group 43

Introduction

The line of ^{125}I sources manufactured by Eckert & Ziegler BEBIG (Berlin, Germany) under the brand name IsoSeed includes models I25.S06 with a gold radio-opaque marker (1, 2) and I25.S17 with a molybdenum radio-opaque marker (3). A variant of the latter model, IsoSeed I25.S17plus, has been designed to essentially replace the molybdenum marker with a silver one. The physics underlying the low-energy regime of ^{125}I photon emissions renders the dosimetric properties of each source design unique. On that basis, the American Association of Physicists in Medicine (AAPM) recommends through the Task Group (TG)-43 (Update 1) report (4) that all new low-energy interstitial brachytherapy seeds should undergo a Monte Carlo (MC)-based and at least one experimental dosimetry characterization before their clinical implementation. In a previous study, the TG-43 dosimetry parameters of the IsoSeed I25.S17plus source were determined using MC simulations (5). In the present study, experimental dosimetry for the I25.S17plus source is performed using LiF thermoluminescent dosimeter (TLD) type TLD-100 dosimeters and two Solid Water (SW) (6) phantoms. Experimental results are compared with corresponding MC calculations for the specific source and results from the literature for seeds of similar design.

Received 14 May 2014; received in revised form 2 July 2014; accepted 2 July 2014.

* Corresponding author. Medical Physics Laboratory, Medical School, National and Kapodestrian University of Athens, 75 Mikras Asias Street, Goudi, 115 27, Athens, Greece. Tel.: +30-210-746-2442; fax: +30-210-746-2369.
E-mail address: ppapagi@med.uoa.gr (P. Papagiannis).

1538-4721/$ - see front matter
http://dx.doi.org/10.1016/j.brachy.2014.07.001

Methods and materials

Source characteristics

The I25.S17plus source design consists of a cylindrical silver rod (3.4 mm length and 0.51 mm diameter) coated with a radioactive silver halide layer. The radioactive silver rod is encapsulated in a hollow titanium tube of 3.7 mm length and 0.8 mm diameter, which is sealed by laser welding using two hemispherical shaped end welds of 0.4 mm thickness each. The external dimensions of the source are 4.5 mm length and 0.8 mm diameter. Further details on the materials and geometric characteristics of the specific source design can be found in the study by Pantelis *et al.* (5) along with the corresponding MC-calculated TG-43 (4) dosimetry parameters. The main difference of the new I25.S17plus ^{125}I seed relative to other seeds provided by the same vendor is the use of Ag as marker material instead of Mo in I25.S17 and Au in I25.S06 seeds (1, 3).

Four seeds were provided by the vendor for the purposes of this experimental study. The air-kerma strength, S_K, of one of the seeds was determined by the National Institute of Standards and Technology (NIST, Gaithersburg, MD) Primary Standard Dosimetry Laboratory using the wide-angle free-air chamber and excluding the Ti K-edge characteristic x-rays (4, 7). The remainder of the seeds (hereafter referred to as Seed 1, Seed 2 and Seed 3) had S_K calibrations of secondary traceability to NIST, established through their calibration by comparison to the seed calibrated at NIST in a series of measurements performed by the manufacturer (4).

Phantom specifications

All measurements were performed in custom phantoms prepared from slabs of SW material (Gammex 457, Gammex Inc., Middleton, WI). The SW slabs were stacked to form a 30-cm^{3}cubic phantom approximating the dimensions of a 15 cm radius spherical liquid-water phantom used in the MC dosimetry calculations for the specific source model (5). Cylindrical cavities of 1.5 mm diameter and 1.0 mm depth were drilled into the central phantom slab to accommodate the TLD microcubes 1 mm^3. The configuration of the cavities was different between the radial dose function and the two-dimensional (2D) anisotropy function measurements, thus resulting in two separate phantom designs (Fig. 1) similar to those previously used for corresponding measurements of different ^{125}I brachytherapy seeds (8–10). In the phantom used for radial dose function measurements (Fig. 1a), cavities were drilled into the central slab for radial distances, r, spanning from 1.00 to 7.00 cm with respect to the source center in 0.50 cm increments exhibiting a spiral configuration to minimize inter-dosimeter attenuation and perturbation effects (8, 10). Four spiral-shaped cavity arrays permitted multiple TLD measurements per radial distance. Measurements of the 1-cm dose rate for evaluation of Λ were performed in the same phantom at r = 1.00 cm. A cylindrical SW insert was used to accommodate the source in the central slab with its longitudinal axis oriented perpendicular to the plane of the slab and its center aligned with the geometric centers of the cavities.

In the phantom used for anisotropy function measurements (Fig. 1b), cavities were drilled in the central slab on concentric cycles of radius r = 1.00, 1.50, 2.00, 3.00, 4.00, 5.00, and 7.00 cm relative to the source center and polar angles θ ranging from 0° to 360° in 30° increments with respect to the source longitudinal axis. For this phantom design, the source was horizontally positioned with its longitudinal axis parallel to the plane of the central slab so that the ends of the source pointed toward 0° and 180°. The 2D anisotropy function measurements were performed with all

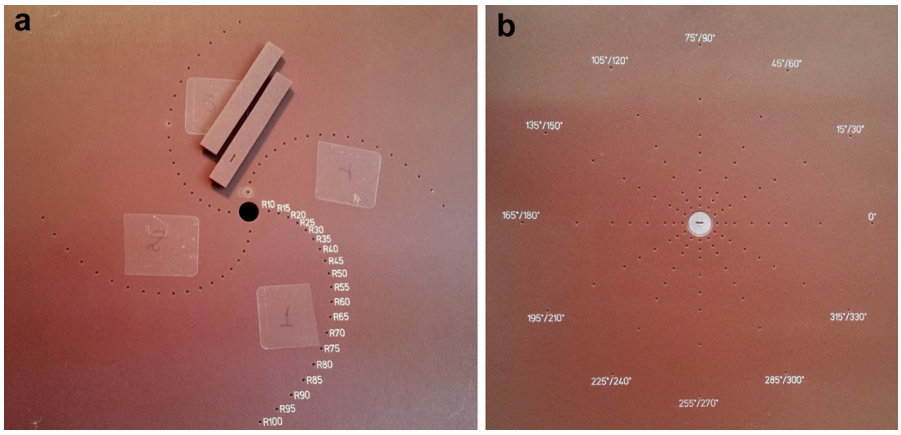

Fig. 1. (a) Photograph of the central phantom slab used for the radial dose function measurements. The cylindrical Solid Water insert used to position the source perpendicular to the slab plane is also depicted. Evaluation of Λ was performed in the same phantom using dose rate measurements at r = 1.00 cm. (b) Photograph of the central phantom slab used for two-dimensional anisotropy function measurements. In this phantom, the source was positioned horizontally with its longitudinal axis parallel to the slab plane and measurements were performed at polar angles θ ranging from 30° to 360° in 30° increments. Rotating the cylindrical Solid Water insert used to position the source by 15° allows for measurements at θ ranging from 15° to 345° in 30° increments. This phantom feature was not used in the present study.

cavities containing a TLD dosimeter, because experimental anisotropy function results at a specific (r,θ) location are not affected considerably by the interposition of dosimeters at the same polar angle, θ, but at smaller distances, r (8).

The use of SW as a phantom material for the experimental dosimetry of low-energy brachytherapy sources is associated with a phantom-to-liquid water correction factor (see TLD response correction section). The mass density of the SW material used for phantom construction was measured equal to 1.04 ± 0.01 g/cm^3 using the small-volume SW pieces for source placement in the phantom and Archimedes principle with a high precision scale (ABT 320-4M, Kern & Sohn GmbH). This value is in excellent agreement with the manufacturer-stated mass density of 1.04 g/cm^3. Besides density, the phantom correction factor also depends on SW elemental composition and especially the Ca content, which has been reported to deviate from manufacturer specifications up to 30% (2). Although associated with a larger phantom correction, (11) low-Z plastic materials, such as PMMA—polymethyl methacrylate, can be used (4) in view of their well-defined elemental composition (10).

In the absence of an independent elemental characterization, SW was used as a phantom material in this work adopting the nominal elemental composition and fraction by weight (H: 8.1%, C: 67.2%, O: 19. %, N: 2.4%, Ca: 2.3%, and Cl: 0.1%). An SW correction factor was determined using MC calculations for the nominal SW composition (see TLD response correction section), and the discrepancies between the nominal and the actual Ca content in SW material reported in the literature were taken into account in the determination of the associated type B (nonstatistical) uncertainty as described in the Uncertainty budget section.

TLD methodology

A batch of 100 LiF type TLD-100 microcubes (Thermo Scientific, Oakwood Village, OH) was used in the present study. The dosimeters were stored in two separate aluminum trays that were also used for the annealing in a Nabertherm (Nabertherm GmbH, Germany) TLD oven. One day before irradiation, TLDs were annealed for 1 h at 400°C and 2 h at 105°C separated by a cooling down procedure to 70°C. After irradiation, the TLDs were stored in room temperature for 24 h, annealed for 10 min at 105°C and allowed to cool down to room temperature before readout, which was performed using a VICTOREEN 2800M hot gas (nitrogen) reader. The time temperature profile was scheduled to start at 60°C and included two 10 s heating steps: the first at 160°C and the second at 300°C. Each irradiated dosimeter was subjected to two sequential readout heating cycles, and the net light output integrated over the entire glow curve was assigned to its response. Readout sessions were carried out in an uninterrupted manner, over a period of almost 4.5 h for each experiment. The TLD-reader system response to a built-in light source containing a ^{14}C (β^-emitter) embedded in a NaI crystal was checked both before and during each readout session, at intervals not exceeding the readout of four dosimeters. The corresponding data were used to fine-tune the photomultiplier high voltage and monitor the stability of the light measuring section and its associated electronics, which was within 2%.

Before the experiments, all TLDs were exposed to 1.00 Gy at a depth of 5.0 cm inside an SW slab phantom using a 6 MV Linac beam collimated to a 20 cm^2 field. A relative sensitivity factor, s_i, was determined for each dosimeter by relating its net reading, $R_{i,\mathrm{net}}$, to the average net response of all dosimeters according to:

$$s_i = \frac{R_{i,\mathrm{net}}}{\frac{1}{n}\sum_{i=1}^{n}\left(R_i - R_i^{bg}\right)}, \quad (1)$$

where n is the total number of the TLDs, and R_i and R_i^{bg} are the integrated light output collected in the first and second readout cycle, respectively, for the ith dosimeter. An ionization chamber array (MatriXX, IBA Dosimetry GmbH, Germany) was used to check the field flatness over the area occupied by the TLDs, and this was found to be better than 1%. The procedure was repeated five times, and the individual precision of each dosimeter was assessed by calculating the standard deviation of the mean s_i values. The TLDs were read in the same order in each readout session to account for any systematic changes in photomultiplier sensitivity or fading of s_i factors during the readout process.

Dose calibration of the TLD response was performed by irradiating 10 sets of eight dosimeters to doses ranging from 0.01 to 2.25 Gy using a 6 MV x-ray beam produced by a Synergy Linac (Elekta AB, Sweden). TLDs were positioned at 5.0-cm depth in an SW slab phantom and irradiated with a 20-cm^2 field defined at the phantom surface, which was positioned at source surface distance (SSD) = 100.0 cm for all calibration dose levels except for 0.01 Gy, where an SSD of 120.0 cm was used for a diminished dose rate. The absorbed dose to water delivered to each TLD was determined using a Farmer-type ionization chamber situated 2.0 cm beneath the slab containing the TLD dosimeters, in alignment with the center of the irradiation field. The attenuation properties of SW are considered equivalent to those of liquid water at 6 MV. TLD response was found to vary linearly with dose for the measured dose range and a linear calibration coefficient, C_{cal}, equal to 0.1418 ± 0.0007 nC/Gy was determined using weighted least squares regression, because each point in the dose-response data set is known with different uncertainty. The weights used were equal to the inverse-squared standard deviation of the mean measured TLD response to each dose level. Concurrent with TLD calibration irradiations, a separate set of 10 control dosimeters was exposed to 1.00 Gy in the same irradiation setup. Irradiations of the specific control dosimeters using the calibration setup were performed in parallel to each experiment to monitor potential changes of the TLD batch

sensitivity (which would translate to changes in the calibration coefficient, C_{cal}). Experimental and control dosimeters were subject to the same thermal history and measured in the same readout session.

Adopting the terminology of a recently introduced formalism, (12) the following formula was applied to determine dose rate in water per unit air-kerma strength, $\dot{D}(r,\theta)/_{S_K}$, from TLD response:

$$\frac{\dot{D}(r,\theta)}{S_K} = P_{\text{phant}}(r,\theta)\cdot\frac{R_{i,\text{net}}\cdot\lambda\cdot f^{\text{rel}}(r,\theta)\cdot k_{bq}^{\text{rel}}}{s_i\cdot S_K\cdot\left(e^{-\lambda t_1}-e^{-\lambda t_2}\right)}\cdot N, \quad (2)$$

where $R_{i,\text{net}}$ is the net TLD response, s_i is the relative sensitivity factor of each dosimeter, $N\ (=1/C_{cal})$ is the absorbed dose calibration coefficient in Gy/nC, λ is the decay constant for ^{125}I, $P(r,\theta)$ is the correction factor accounting for the use of SW phantom material, f^{rel} is the TLD relative absorbed dose energy dependence with respect to the 6 MV calibration beam, k_{bq}^{rel} is the corresponding relative intrinsic energy dependence of TLDs (see TLD response correction section), and t_1 and t_2 are the time points of TLD placement and removal, respectively.

Experimental results for the radial dose function, $g(r)$, were obtained by averaging TLD measurements at the same r. For the 2D anisotropy function, $F(r,\theta)$, measurements from TLDs lying at corresponding (r,θ) coordinates in each phantom quadrant were averaged. For the determination of both $g(r)$ and $F(r,\theta)$ values, the line-source approximation of the geometry function was used (4).

Irradiation details

TLD dosimeters were loaded in each phantom before seed placement. A total of 82 dosimeters were selected for the measurements based on reproducibility (precision $\leq$ 3%) criteria. Measurements of $g(r)$ for each seed were performed over a 72 h time period to provide a dose >0.01 Gy at 5.00 cm. For this irradiation duration, the four dosimeters positioned at r = 1.00 cm were replaced twice in a 24 h interval, resulting in 12 measurements of Λ for each seed. Before replacing the dosimeters, the source was removed from the phantom and subsequently repositioned. This approach randomized the effect of potential seed-TLD positioning uncertainties on the experimental results.

$F(r,\theta)$ measurements were performed for $r \leq$ 5.00 cm over 96 h for each seed. TLDs at r = 1.00 cm, except for those at $\theta = 0^\circ$ and $\theta = 180^\circ$, were replaced 24 h after seed placement. This practice resulted in an additional set of $F(r,\theta)$ measurements at r = 1.00 cm and $\theta = 30^\circ$ and 60° for each phantom quadrant.

TLD response correction

The AAPM TG-43 formalism is based on brachytherapy source dosimetry parameters evaluated in liquid water (4, 13). Therefore, TLD measurements of this work were corrected to account for the use of SW as phantom material. The corresponding correction factor, $P_{\text{phant}}(r,\theta)$, was estimated by the following ratio:

$$P_{\text{phant}}(r,\theta) = \left[\frac{D_w^w(r,\theta)}{D_w^{SW}(r,\theta)}\right]_{^{125}\text{I}}, \quad (3)$$

where $D_w^w(r,\theta)$ and $D_w^{SW}(r,\theta)$ are the dose to water at (r,θ) in the absence of the detector in liquid water and SW phantom material, respectively, for the ^{125}I source.

Moreover, because the TLDs were calibrated in terms of absorbed dose to water using a 6 MV x-ray photon beam, the different absorbed dose energy dependence of the TLDs in the ^{125}I beam quality, $f^{^{125}\text{I}}$, must be taken into account. This was done using the relative absorbed dose energy dependence coefficient, f^{rel}, which was estimated by the following formula:

$$f^{\text{rel}}(r,\theta) = \frac{f^{6\text{MV}}(r,\theta)}{f^{^{125}\text{I}}(r,\theta)} = \frac{\left[D_w^w/D_{\text{TLD}}^w\right]^{6\text{MV}}}{\left[D_w^w(r,\theta)/D_{\text{TLD}}^w(r,\theta)\right]^{^{125}\text{I}}}, \quad (4)$$

where $D_{\text{TLD}}^w(r,\theta)$ is the average dose in a TLD centered at (r,θ) and $D_w^w(r,\theta)$ is the dose to water at the midpoint of the detector at (r,θ) in the absence of the detector assuming a point detector approximation, that is a 0.1 mm^3 voxel. The corresponding ratio $\left[D_w^w/D_{\text{TLD}}^w\right]^{6\text{MV}}$ refers to the calibration beam energy and irradiation geometry. It is noted that, the different attenuation properties of TLD material relative to water and the volume averaging effects induced by the finite detector dimensions at low energies are included in f^{rel} values obtained using Eq. 4 because both detector material composition and dimensions were considered for the determination of D_{TLD}^w at ^{125}I photon energies. To facilitate direct comparison with corresponding data reported in the literature, results and discussion of this work will hereafter refer to the inverse of the relative absorbed dose energy dependence, $(f^{\text{rel}})^{-1}$.

$P_{\text{phant}}(r,\theta)$ and $f^{\text{rel}}(r,\theta)$ values were determined using the MCNP v.6.1 general purpose MC code (14) and the mcplib04 photoatomic cross-section library, which is based on the Lawrence Livermore National Laboratory (Livermore, CA)- evaluated photon data library (1997 version). MC simulations were performed for the nominal geometry and material composition of the model I125.S17plus seed described in detail by Pantelis *et al.* (5) using the ^{125}I energy spectrum recommended by the TG-43U1 report (4). The absorbed dose was approximated by collisional kerma and calculated using a *FMESH4:p tally. Specific to each detector material simulated, an FM card was used to transform the tally output into collisional kerma using the corresponding mass-energy absorption coefficients, μ_{en}/ρ, taken from XCOM (15). For the TLD dosimeters, the μ_{en}/ρ coefficients for LiF were used because μ_{en}/ρ coefficients of

LiF:Mg,Ti and LiF were found to differ by 0.3% for photon energies <30 keV. Only photons were simulated and a 1 keV photon energy cutoff was used. Calculation of D^{w}_{TLD} in the I25.S17plus photon energies was performed in a 100 × 100 × 1 mm^3 rectangular mesh grid of 1 mm^3 bin size. Results were corrected a posteriori for the 2.58%, position independent, effect of the different attenuation properties of LiF material relative to water, based on results of ad hoc MC simulations for individual dosimeters placed at (r,θ) positions corresponding to the experimental setup. D^{125I}_{w} calculations were performed in a cylindrical mesh grid aligned with the sources' longitudinal axis, consisting of 0.1 mm^2 cylindrical rings for radial distances up to 50.0 mm and 1 mm^2 for $50.0 \leq r \leq 100.0$ mm. Linear interpolations were performed on the MC-calculated data to obtain the correction factor values at the location of each experimental point.

For the 6 MV x-ray photon beam quality, D^{w}_{TLD} and D^{w}_{w} were calculated using the *F8:p,e pulse height tally. Fully coupled photon-electron transport with photon and electron energy cutoffs of 1 keV and 10 keV were used for the simulations, respectively. A point-source model of 6 MV x-ray photons was simulated using the photon spectrum data reported by Sheikh-Bagheri and Rogers (16) for the specific linac model used in this work (the water phantom surface was placed 100 cm from the linac source).

A total of 5×10^{10} and 5×10^{9} photon histories were simulated for the I25.S17plus seed and the 6 MV irradiations, respectively.

Finally, recent work has demonstrated an additional component of TLD-100 energy dependence that cannot be calculated using MC simulation (17–21). This intrinsic energy dependence, defined as the ratio of the dose to the detector to the detector's reading (after properly corrected for influence parameters) in a given beam quality, arises from the solid-state nature of the TLD dosimeters and can be a 13% effect at photon energies ranging from 12 keV to 145 keV (19). In the present study, the different intrinsic energy dependence of TLDs in the ^{125}I irradiation relative to the calibration beam quality (6 MV) was accounted for using the factor k^{rel}_{bq} presented in Eq. 4. A k^{rel}_{bq} value of 0.916 (with an uncertainty of 2.5% at $k = 1$) was adopted from the work of Kennedy *et al*. (10), in view of the same TLD type and geometry used, the comparable quality of ^{60}Co and 6 MV x-ray beams, and the results announced by Rasmussen *et al*. (17), according to which this correction factor was largely independent from the irradiation geometry and source-to-source variability. Because the values of both $g(r)$ and $F(r,\theta)$ are relative, the intrinsic energy dependence correction was applied only to the Λ results.

Uncertainty budget

Uncertainties associated with the experimental determination of Λ for the NIST-calibrated seed are presented in Table 1. Uncertainty values are reported using a coverage factor $k = 1$ (i.e., 1σ) to facilitate direct comparison with the AAPM TG-43U1 recommendations (4), according to which brachytherapy dosimetry measurements should be performed using a detector with sufficient precision and reproducibility to permit dose estimation with 1σ type A (statistical) uncertainties ≤ 5% and 1σ type B (nonstatistical) uncertainties ≤ 7%. The type A uncertainty assigned to repetitive TLD measurements was estimated from the standard deviation of the mean value. The uncertainty associated with the TLD dose calibration procedure included the determination of absorbed dose to water, positioning of TLDs in the reference depth, and the combined effect of TLD reproducibility and reader stability. The uncertainty in absorbed dose-to-water measurement using a Farmer-type ionization chamber was estimated following the recommendations of the TRS-398 code of practice (22). The uncertainty of k^{rel}_{bq} is taken from the work of Kennedy *et al*. (10). The type B uncertainty assigned to the phantom correction factor, P_{phant}, was estimated by the combined effect of uncertainties in the density and the elemental composition of the SW phantom material and the uncertainty of the photoatomic cross-sections used by the specific MC code used in this work. Separate MC runs of varying SW density showed that the corresponding effect on P_{phant} is <0.3% for density variations of up to 2% (i.e., twice the uncertainty of the measured SW density at $k = 1$). Regarding SW elemental composition, an uncertainty contribution of 2.4% was estimated by assuming a rectangular distribution of minimum and maximum P_{phant} values equal to those presented in the study by Meigooni *et al*. (23) for the lower and higher Ca content compositions reported in the literature. Results from the study by Meigooni *et al*. (23) were obtained using the MCNP5 code with updated photoatomic cross-section libraries and an SW material density similar to that measured in this study. The type B component due to the cross-section libraries was

Table 1
Analysis of the uncertainty associated with TLD results for the dose-rate constant of the I25.S17plus brachytherapy source

Component	Type A (%)	Type B (%)
Average of repetitive measurements	3.22[a]	—
TLD dose calibration	0.48	1.21
Relative intrinsic energy dependence, k^{rel}_{bq}		2.50
Phantom material correction factor, P_{phant}	0.14	2.46
Relative absorbed dose energy dependence, f^{rel}	0.56	1.0
TLD-source relative positioning		0.6
Source strength, S_K		0.78[b]
Quadratic sum	3.31	3.97
Combined total uncertainty ($k = 1$)	5.16[c]	

TLD = thermoluminescent dosimeter.

Random or statistical effects are described with type A uncertainties, whereas type B uncertainties account for nonstatistical discrepancies. The tabulated values correspond to the National Institute of Standards and Technology–calibrated seed.

[a] 3.20%, 5.90%, and 3.44% for seed 1, 2, and 3, respectively.

[b] 1% for seed 1, 2, and 3.

[c] 5.19%, 7.18%, and 5.34% for seed 1, 2, and 3, respectively.

estimated to be equal to 0.6% by reviewing P_{phant} results in the literature for the same SW elemental composition obtained using different MC codes (8, 11, 23, 24). The type B uncertainty assigned to the relative absorbed dose energy dependence, f^{rel}, stems from a corresponding uncertainty in the mass-energy absorption coefficients used (25). The uncertainty assigned to TLD-source relative positioning was estimated assuming a rectangular distribution and taking into account the 0.05 mm machining tolerance of the SW phantom reported by the manufacturer. The uncertainty of the air-kerma strength, S_K, was taken from the NIST source calibration certificate. The corresponding uncertainty for seeds 1, 2, and 3 was greater because it also includes the calibration uncertainty of the well-type chamber used by the source vendor. It is noted that the uncertainties associated with the determination of the source strength, S_K, and the TLD calibration procedure do not affect experimental results for radial dose and anisotropy function.

Results and discussion

TLD response factor

Figure 2a presents MC-calculated results for the correction factor $P_{phant}(r,\theta)$ accounting for the use of the specific SW phantom material in TLD measurements of this work. $P_{phant}(r,\theta)$ data are plotted as a function of radial distance for polar angles $\theta = 0°$, 30°, 60°, and 90°. As clearly seen, apart from $\theta = 0°$, $P_{phant}(r,\theta)$ is essentially independent of θ and increases linearly with r according to: $P_{phant}(r) = (0.0423 \pm 0.0003)\ r + (0.9827 \pm 0.0014)$. For $\theta = 0°$, Fig 2a results suggest that $P_{phant}(r,90°)$ is still linearly dependent on r, yet almost 3% greater than corresponding $P_{phant}(r,\theta \neq 0°)$ values.

At $(r_0, \theta_0) = (1\text{ cm}, 90°)$, a P_{phant} value of 1.025 was obtained, which is 0.6% lower than that reported recently by Meigooni *et al.* (23) for the same SW atomic composition and similar density and almost 2% lower corresponding results previously published in the literature (8, 11, 24, 26, 27). Besides comparison to published data, the $P_{phant}(1\text{ cm}, 90°)$ of this work was further corroborated through additional MC simulations for a point source with an emitted photon spectrum of pure ^{125}I (4) and that of an ^{125}I source containing Ag (26), which yielded results within type A simulation uncertainties.

The inverse of the MC-calculated relative absorbed dose energy dependence values, $(f^{rel})^{-1}$, are plotted in Fig 2b as a function of radial distance for $\theta = 0°$, 30°, 60°, and 90°. Except for $\theta = 0°$, $[f^{rel}(r,\theta)]^{-1}$ was found to be essentially constant with an average value of 1.406 ± 0.008 ($k = 1$). This value is in agreement, within uncertainties, with corresponding $(f^{rel})^{-1}$ data published in the literature (3, 8, 26, 28, 29). At points lying along the longitudinal source axis ($\theta = 0°$), an abrupt decrease as a function of r was observed. This is attributed to volume averaging effects in the finite TLD dimensions, which were considered in f^{rel} calculations of this study. As r value increases, volume averaging is reduced and $[f^{rel}(r,0°)]^{-1}$ gradually attains an average value of 1.440 ± 0.028 ($k = 1$), which is 2.6% greater than the corresponding average $(f^{rel})^{-1}$ value for points lying at $\theta \neq 0°$. This observation is in agreement with corresponding P_{phant} results for $\theta = 0°$ relative to those for $\theta \neq 0°$ and could be attributed to an apparent softening of the ^{125}I source photon energy spectrum at $\theta = 0°$ estimated in this work using a 1-mm sampling resolution, due to the heavy attenuation of radiation emitted from the source core by the end welds of its encapsulation and the concomitant increase of the relative contribution from photons scattered in water along $\theta = 0°$.

Dose-rate constant

Table 2 presents TLD-measured results for the dose-rate constant, Λ, of the I25.S17plus seeds used in the present study. According to the tabulated data, a Λ value equal to 0.944 ± 0.049 cGy h^{-1} U^{-1} ($k = 1$) was measured for the NIST-calibrated seed. This value is in agreement within type A uncertainties, with corresponding results obtained

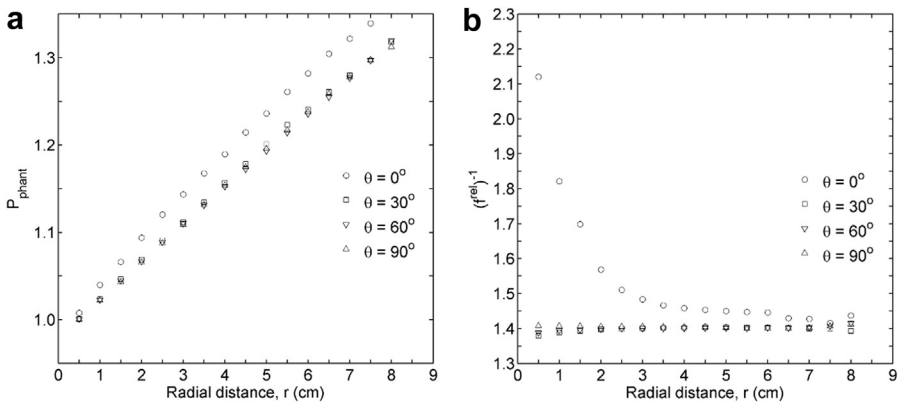

Fig. 2. (a) The MC-calculated phantom correction factor, P_{phant}, used in this work and (b) the inverse of the MC-calculated relative absorbed-dose energy-dependence, $(f^{rel})^{-1}$, for the type TLD-100 dosimeters used. Both data sets are plotted vs. radial distance, r, from the center of the I25.S17plus source and for polar angles, $\theta = 0°$, 30°, 60°, and 90°.

Table 2
TLD results obtained in this work for the dose rate constant, Λ, of the I25.S17plus brachytherapy source

Method	Λ (cGy h^{-1} U^{-1})
TLD—NIST calibrated seed	0.944 ± 0.049
TLD—seed 1	0.942 ± 0.049
TLD—seed 2	0.984 ± 0.070
TLD—seed 3	0.952 ± 0.051
MC_{WAFAC}	0.925 ± 0.019

TLD = thermoluminescent dosimeter; NIST = National Institute of Standards and Technology; MC = Monte Carlo; WAFAC = wide-angle free-air chamber.

The corresponding MC value for the same source published by Pantelis *et al*. (5) is also included for comparison. The presented total absolute uncertainties correspond to $k = 1$.

from the rest of the four seeds with S_K calibrations of secondary NIST traceability. Collectively, a mean Λ of 0.956 ± 0.043 cGy h^{-1} U^{-1} ($k = 1$) was determined for the I25.S17plus source, which agrees within uncertainties with the MC-calculated dose-rate constant of: Λ_{MC} = 0.925 ± 0.013 cGy h^{-1} U^{-1} ($k = 1$) published by Pantelis *et al*. (5).

Measured Λ values for seeds of similar design as I25.S17plus seed are 0.938 ± 0.065 cGy h^{-1} U^{-1}, 0.921 ± 0.055 cGy h^{-1} U^{-1}, and 0.940 ± 0.055 cGy h^{-1} U^{-1} for the selectSeed (8) and the model 6711 (10) and 9011 (10) sources, respectively. The photon spectrometry-measured Λ value for the AgX100 brachytherapy source is 0.957 ± 0.037 cGy h^{-1} U^{-1} (26). All these results are in agreement within experimental uncertainties with the TLD-measured Λ value of the present study. Relative to ^{125}I brachytherapy source models available from the same vendor, the measured Λ value for the I25.S17plus seed agrees within type A uncertainties with the TLD-measured value of 0.951 ± 0.044 cGy h^{-1} U^{-1} ($k = 1$) for the I25.S17 source having a Mo marker (3) and is lower by 10% relative to that for the I25.S06 source having an Au marker (2), in accordance with the corresponding MC based findings of our previous work (5).

Radial dose and anisotropy functions

Table 3 presents TLD-measured radial dose function results, $g(r)$, for the model I125.S17plus source, reported using the line-source geometry function (4) and obtained through averaging of corresponding measurements for each seed. Corresponding MC calculations (5) and the consensus $g(r)$ data for the model 6711 brachytherapy source published in the AAPM TG-43U1 report (4) are included in Table 3 for comparison. The measured and simulated $g(r)$ results for the model I125.S17plus source are also presented in Fig. 3. As seen both in Table 3 and Fig. 3 data, TLD and MC-calculated results for the model I125.S17plus source were found to agree within uncertainties for $r \leq 5.00$ cm. For $6.00 \leq r \leq 7.00$ cm, the TLD-measured values were greater than the corresponding MC

Table 3
TLD radial dose function results, $g(r)$, obtained in the present study by averaging corresponding data from the four seeds used

	Radial dose function, $g(r)$		
	I25.S17plus		6711
Radial distance (cm)	TLD	MC	Consensus
1.00	1.000	1.000	1.000
1.50	0.938 (36)	0.909 (27)	0.908
2.00	0.828 (30)	0.814 (24)	0.814
2.50	0.734 (26)	0.722 (21)	…
3.00	0.654 (24)	0.635 (19)	0.632
3.50	0.552 (28)	0.555 (16)	…
4.00	0.505 (18)	0.482 (14)	0.496
4.50	0.437 (16)	0.419 (12)	…
5.00	0.378 (14)	0.363 (11)	0.364
5.50	0.330 (12)	…	…
6.00	0.291 (11)	0.270 (08)	0.270
6.50	0.247 (11)	…	…
7.00	0.218 (08)	0.199 (06)	0.199

TLD = thermoluminescent dosimeter; MC = Monte Carlo.

Corresponding MC-calculated results by Pantelis *et al*. (5) for the same source and consensus data obtained from the Task Group-43U1[4] report for the model 6711 seed are also presented for comparison. Total absolute uncertainties ($k = 1$) are given in parenthesis.

results, yet within the expanded uncertainties ($k = 2$). Similar findings were deduced from the comparison of the measured $g(r)$ results for the model I125.S17plus source to the corresponding consensus data for the model 6711 brachytherapy source, which exhibits similar design characteristics (30).

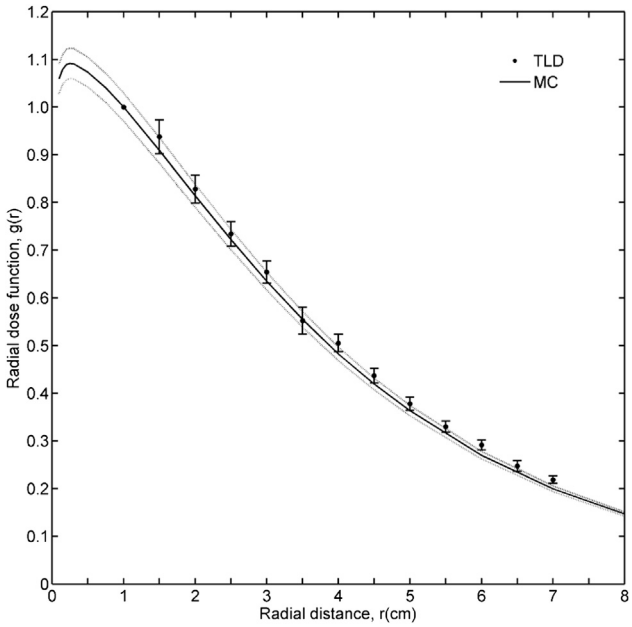

Fig. 3. TLD-measured and MC-calculated results for the radial dose function, $g(r)$, of the I25.S17plus source. The error bars on the TLD-measured data correspond to the combined total experimental uncertainties at $k = 1$. The dotted lines indicate the confidence intervals of MC-calculated results also at $k = 1$.

Table 4
TLD anisotropy function results, $F(r,\theta)$, obtained in the present study by averaging corresponding data from the four seeds used

Radial distance (cm)	Polar angle (degrees)	Anisotropy function, $F(r,\theta)$	
		TLD	MC
1.00	0	0.325 (19)	0.287 (16)
	30	0.860 (51)	0.832 (26)
	60	1.007 (52)	1.017 (30)
	90	1.000	1.000
1.50	0	0.395 (23)	0.347 (15)
	30	0.833 (50)	0.842 (26)
	60	0.971 (64)	1.009 (30)
	90	1.000	1.000
2.00	0	0.432 (28)	0.400 (16)
	30	0.832 (43)	0.849 (26)
	60	0.997 (47)	1.004 (30)
	90	1.000	1.000
3.00	0	0.523 (24)	0.469 (19)
	30	0.850 (36)	0.858 (26)
	60	1.012 (46)	0.997 (30)
	90	1.000	1.000
4.00	0	0.536 (27)	0.473 (19)
	30	0.828 (55)	0.865 (26)
	60	0.991 (40)	0.997 (30)
	90	1.000	1.000
5.00	0	0.585 (23)	0.556 (22)
	30	0.858 (35)	0.866 (26)
	60	0.994 (41)	0.989 (29)
	90	1.000	1.000

TLD = thermoluminescent dosimeter; MC= Monte Carlo.

Corresponding MC values calculated by Pantelis *et al.* (5) are also presented for comparison. Total absolute uncertainties ($k = 1$) are given in parenthesis.

The average TLD-measured $F(r,\theta)$ results, calculated using the line-source geometry function (4) are presented in Table 4 along with corresponding MC estimated values. TLD-measured and MC-calculated results agreed within tabulated uncertainties ($k = 1$) for all radial distances and polar angles, except for points lying at $\theta = 0°$, where TLD measurements yield $F(r,0°)$ values systematically greater by up to 14% at $r = 1.5$ cm.

Conclusions

This study describes the first experimental study of the model I25.S17plus brachytherapy source in terms of TG-43 dosimetry parameters. Agreement within uncertainties was found with corresponding results obtained independently using MC simulations and corresponding results in the literature for sources having similar designs incorporating a silver marker.

Acknowledgments

This work was supported in part by a research grant provided by Eckert & Ziegler BEBIG GmbH.

Michael Andrássy, senior physicist and Sabrina Oertel, product manager at Eckert & Ziegler BEBIG GmbH are gratefully acknowledged for information exchange and arrangement of the delivery of the radioactive sources.

References

[1] Hedtjärn H, Carlsson GA, Williamson JF. Monte Carlo-aided dosimetry of the Symmetra model I25.S06 ^{125}I, interstitial brachytherapy seed. *Med Phys* 2000;27:1076–1085.

[2] Patel NS, Chiu-Tsao S-T, Williamson JF, *et al*. Thermoluminescent dosimetry of the Symmetra^{TM} ^{125}I model I25.S06 interstitial brachytherapy seed. *Med Phys* 2001;28:1761–1769.

[3] Lymperopoulou G, Papagiannis P, Sakelliou L, *et al*. Monte Carlo and thermoluminescence dosimetry of the new IsoSeed model I25.S17 ^{125}I interstitial brachytherapy seed. *Med Phys* 2005;32:3313–3317.

[4] Rivard MJ, Coursey BM, DeWerd LA, *et al*. Update of AAPM Task Group No. 43 Report: A revised AAPM protocol for brachytherapy dose calculations. *Med Phys* 2004;31:633–673.

[5] Pantelis E, Papagiannis P, Anagnostopoulos G, *et al*. New ^{125}I brachytherapy source IsoSeed I25.S17plus: Monte Carlo dosimetry simulation and comparison to sources of similar design. *J Contemp Brachytherapy* 2013;5:240–249.

[6] Constantinou C. A solid water phantom material for radiotherapy x-ray and γ-ray beam calibrations. *Med Phys* 1982;9:436–441.

[7] Williamson JF, Coursey BM, DeWerd LA, *et al*. Guidance to users of Nycomed Amersham and North American Scientific, Inc., I-125 interstitial sources: Dosimetry and calibration changes: Recommendations of the American Association of Physicists in Medicine Radiation Therapy Committee Ad Hoc Subcommittee. *Med Phys* 1999;26:570–573.

[8] Anagnostopoulos G, Baltas D, Karaiskos P, *et al*. Thermoluminescent dosimetry of the selectSeed ^{125}I interstitial brachytherapy seed. *Med Phys* 2002;29:709–716.

[9] Meigooni AS. Instrumentation and dosimeter-size artifacts in quantitative thermoluminescence dosimetry of low-dose fields. *Med Phys* 1995;22:555–561.

[10] Kennedy RM, Davis SD, Micka JA, *et al*. Experimental and Monte Carlo determination of the TG-43 dosimetric parameters for the model 9011 THINSeed^{TM} brachytherapy source. *Med Phys* 2010;37:1681–1688.

[11] Luxton G. Comparison of radiation dosimetry in water and in solid phantom materials for I-125 and Pd-103 brachytherapy sources: EGS4 Monte Carlo study. *Med Phys* 1999;21:631–641.

[12] Rogers DWO. General characteristics of radiation dosimeters and a terminology to describe them. In: Rogers DWO, Cygler JE, editors. *Clinical dosimetry measurements in radiotherapy.* Madison, WI: Medical Physics Publishing; 2009. p. 137–145.

[13] Nath R, Anderson LL, Luxton G, *et al*. Dosimetry of interstitial brachytherapy sources: Recommendations of the AAPM Radiation Therapy Committee Tasks Group No. 43. *Med Phys* 1995;22:209–234.

[14] Goorly T, James M, Booth T, *et al. Initial MCNP6 Release Overview—MCNP6 version 1.0.* Available at: https://laws.lanl.gov/vhosts/mcnp.lanl.gov/pdf_files/la-ur-13-22934.pdf. Accessed May 9, 2014.

[15] Hubbell JH, Seltzer SM. *Tables of x-ray mass attenuation coefficients and mass energy absoprtion coefficients (version 1.4).* Gaithersburg, MD: National Institute of Standards and Technology; 2004. [Online] Available at: http://physics.nist.gov/xaamdi. Accessed 30-Mar-2014.

[16] Sheikh-Bagheri D, Rogers DWO. Monte Carlo calculation of nine megavoltage photon beam spectra using the BEAM code. *Med Phys* 2002;29:391–402.

[17] Rasmussen B, Davis S, Micka J, *et al*. SU-GG-T-292: The response of LiF:Mg,Ti thermoluminescent dosimeters to low-energy photons. *Med Phys* 2008;35:2792.

[18] Hranitzky C, Stadtmann H, Olko P. Determination of LiF:Mg,Ti and LiF:Mg,Cu,P TL efficiency for X-rays and their application to Monte

Carlo simulations of dosemeter response. *Radiat Prot Dosimetry* 2006;119:483–486.

[19] Nunn AA, Davis SD, Micka JA, *et al*. LiF:Mg,Ti TLD response as a function of photon energy for moderately filtered x-ray spectra in the range of 20–250 kVp relative to ^{60}Co. *Med Phys* 2008;35: 1859–1869.

[20] Davis SD, Ross CK, Mobit PN, *et al*. The response of lif thermoluminescence dosemeters to photon beams in the energy range from 30 kV x rays to ^{60}Co gamma rays. *Radiat Prot Dosimetry* 2003; 106:33–43.

[21] Tedgren AC, Hedman A, Grindborg JE, *et al*. Response of LiF:Mg,Ti thermoluminescent dosimeters at photon energies relevant to the dosimetry of brachytherapy (<1 MeV). *Med Phys* 2011;38: 5539–5550.

[22] Andreo P, Burns DT, Hohlfeld K, *et al*. *Absorbed dose determination in external beam radiotherapy.* Vienna, Austria: International Atomic Energy Agency (IAEA); 2000. Technical Report Series No. 398.

[23] Meigooni AS, Awan SB, Thompson NS, *et al*. Updated Solid Water™ to water conversion factors for ^{125}I and ^{103}Pd brachytherapy sources. *Med Phys* 2006;33:3988–3992.

[24] Williamson JF. Comparison of measured and calculated dose rates in water near I-125 and Ir-192 seeds. *Med Phys* 1991;18:776–786.

[25] Andreo P, Burns DT, Salvat F. On the uncertainties of photon mass energy-absorption coefficients and their ratios for radiation dosimetry. *Phys Med Biol* 2012;57:2117–2136.

[26] Chen Z, Bongiorni P, Nath R. Experimental characterization of the dosimetric properties of a newly designed I-Seed model AgX100 ^{125}I interstitial brachytherapy source. *Brachytherapy* 2012;11: 476–482.

[27] Tailor R, Tolani N, Ibbott GS. Thermoluminescence dosimetry measurements of brachytherapy sources in liquid water. *Med Phys* 2008; 35:4063–4069.

[28] Papagiannis P, Sakelliou L, Anagnostopoulos G, *et al*. On the dose rate constant of the selectSeed ^{125}I interstitial brachytherapy seed. *Med Phys* 2006;33:1522–1523.

[29] Popescu CC, Wise J, Sowards K, *et al*. Dosimetric characteristics of the Pharma Seed™ model BT-125-I source. *Med Phys* 2000;27: 2174–2181.

[30] Dolan J, Li Z, Williamson JF. Monte Carlo and experimental dosimetry of an ^{125}I brachytherapy seed. *Med Phys* 2006;33:4675–4684.